energies

MDPI

Article

A Comparative Study of Optimal PV Allocation in a Distribution Network Using Evolutionary Algorithms†

Wenlei Bai [1,*], Wen Zhang [2], Richard Allmendinger [3], Innocent Enyekwe [1] and Kwang Y. Lee [1]

[1] School of Engineering and Computer Science, Baylor University, Waco, TX 76706, USA; innocent_enyekwe1@baylor.edu (I.E.); kwang_y_lee@baylor.edu (K.Y.L.)
[2] Hankamer School of Business, Baylor University, Waco, TX 76706, USA; wen_zhang1@baylor.edu
[3] Alliance Manchester Business School, University of Manchester, Manchester M15 6PB, UK; richard.allmendinger@manchester.ac.uk
* Correspondence: wenlei_bai@baylor.edu
† This paper is an extended version of our paper "Optimal Allocation of PV Systems on Unbalanced Networks Using Evolutionary Algorithms", which was presented at the conference 2023 IEEE Symposium Series on Computational Intelligence (SSCI), Mexico City, Mexico, published on IEEEXplore on 1 January 2024.

Abstract: The growing distributed energy resource (DER) penetration into distribution networks, such as through residential and commercial photovoltaics (PV), has emerged through a transition from passive to active networks, which takes the complexity of planning and operations to the next level. Optimal PV allocation (sizing and location) is challenging because it involves mixed-integer non-linear programming with three-phase non-linear unbalanced power flow equations. Meta-heuristic algorithms have proven their effectiveness in many complex engineering problems. Thus, in this study, we propose to achieve optimal PV allocation by using several basic evolutionary algorithms (EAs), particle swarm optimization (PSO), artificial bee colony (ABC), differential evolution (DE), and their variants, all of which are applied for a study of their performance levels. Two modified unbalanced IEEE test feeders (13 and 37 bus) are developed to evaluate these performance levels, with two objectives: one is to maximize PV penetration, and the other is to minimize the voltage deviation from 1.0 p.u. To handle the computational burden of the sequential power flow and unbalanced network, we adopt an efficient iterative load flow algorithm instead of the commonly used and yet highly simplified forward–backward sweep method. A comparative study of these basic EAs shows their general success in finding a near-optimal solution, except in the case of the DE, which is known for solving continuous optimization problems efficiently. From experiments run 30 times, it is observed that PSO-related algorithms are more efficient and robust in the maximum PV penetration case, while ABC-related algorithms are more efficient and robust in the minimum voltage deviation case.

Keywords: distributed energy resources; evolutionary algorithms; optimal PV allocation; PV penetration

Citation: Bai, W.; Zhang, W.; Allmendinger, R.; Enyekwe, I.; Lee, K.Y. A Comparative Study of Optimal PV Allocation in a Distribution Network Using Evolutionary Algorithms. *Energies* **2024**, *17*, 511. https://doi.org/10.3390/en17020511

Academic Editor: Angela Russo

Received: 9 November 2023
Revised: 6 January 2024
Accepted: 12 January 2024
Published: 20 January 2024

1. Introduction

The high penetration of distributed energy resources (DERs) into distribution networks has positive impacts on the environment, system reliability, and flexibility, yet it also brings challenges from operation and planning perspectives [1]. Today, the distribution network has become more active in the sense of exchanging energy, decentralizing control so it is local and occurs almost in real time, and is continuously developing distributed energy resource (DER) technologies and information and communication technologies (ICT) [2]. The IEEE 1547-2018 standard was released in 2018 to assist with the high penetration of DERs, which launched a new era for DER planning and management [3]. Photovoltaic (PV) systems are among the popular DERs considered by planners thanks to their flexibility, scalability, low operational costs, and mitigation of a demand peak [4]. Yet, PV systems can also bring challenges. One major challenge is that they can cause rapid voltage changes in

the network, especially during sudden changes in solar irradiance. Maintaining voltage within acceptable limits thus becomes a challenge. To overcome this, the optimal allocation of PV systems in terms of location and size is critical for planners.

Distributed power flow, invented in the 1990s [5], is the fundamental tool used to ensure that the allocation of DERs does not violate operating limits such as the node voltage and line current flow. The Newton Raphson method is widely used to solve power flow problems in transmission networks and has recently been adopted for distribution networks [6]. Yet, the computational cost is high due to the Jacobian matrix inversion at each iteration. Another popular and well-known method, backward/forward sweep, was proposed in the early 1990s [5]; however, one of the obvious drawbacks is that it only fits a balanced network. In this work, a simple yet efficient fixed-point method is adopted to tackle three-phase unbalanced load flow. The fixed-point method models power conversion elements (generators, loads) as Norton current equivalent circuits such that node voltages can be solved iteratively with a constant system admittance matrix. In other words, the matrix inversion is calculated only one time and it can solve very unbalanced networks [7]. Details are provided in the Problem Formulation section of this article.

The PV allocation problem can be considered a variant of the optimal power flow (OPF) problem, where the objectives are to maximize PV penetration or minimize the voltage deviation from 1.0 per unit (p.u.) in distribution networks. Per unit (p.u.) is a dimensionless quantity used in power system analysis to normalize various electrical quantities to a common base value. It allows for a more convenient and consistent representation of system parameters and facilitates comparisons between different parts of the power system. The PV allocation problem essentially involves mixed-integer non-linear programming (MINLP), which is hard to carry out with traditional mathematical approaches. The objective of classical OPF is to determine a set of control variables that optimize a certain objective function while satisfying a set of constraints, such as power flow equations, voltage limits, and generator capacity limits [8]. However, in practical power systems, there are various sources of uncertainty, such as load variations, renewable energy generation, and transmission line outages, that make it difficult to accurately predict the system behavior. Bienstock et al. [9] proposed a chance-constrained OPF (CCOPF) formulation for transmission networks that incorporates risk-aware decision making under uncertainty. The CCOPF framework involves optimizing the control variables while satisfying a set of probabilistic constraints that ensure that the system operates within acceptable risk levels. The authors formulated the CCOPF problem as a mixed-integer linear programming (MILP) model, which can be efficiently solved using existing optimization solvers. Nammouchi et al. [10], meanwhile, proposed a novel and robust opportunistic optimization approach, where a conditional value-at-risk (CVaR) measure is employed to capture the impact of uncertainties on the microgrid's operation. The objective in this article, however, is to evaluate the performances of EAs for a variant of OPF in a distribution network, and thus, it is assumed that the load and PV output are known. In other words, uncertainty has not been considered.

Acharya et al. [11] suggested an analytical expression to optimize the size and the location of a single DG. In [12], an analytical approach was also used to optimize the allocation of the DG, to minimize the power loss of the distribution system. However, the analytical-based optimization approach could only give a solution for a single DER effectively. Recently, meta-heuristic methods have proven their effectiveness in complex engineering problems [8,13,14]. Janamala and Rani [15] recently implemented meta-heuristics with the Archimedes optimization algorithm (AOA) to solve the optimal allocation problem. Kumawat et al. [16] proposed a modified group experience with the teaching–learning-based (TLB) optimization approach to address the optimal planning of DERs in harmonic-polluted systems. Furthermore, Nogueira, Negrete, and Lezama [17] conducted a comparative study between PSO and symbiotic organism search (SOS) to determine the size and locations of the DERs using interval power flow. The well-known no free lunch theorem states that no meta-heuristic algorithm can be superior to other algorithms for all optimization problems

universally [18]. Therefore, one of the goals of this work is to explore the effectiveness of the well-known EAs artificial bee colony (ABC), particle swarm optimization (PSO), differential evolution (DE), and their variants for PV allocation problems. The work is an extension of our work in [19], such that additional test cases and more comprehensive study are conducted. In addition, we implement the fix-point method to calculate the unbalanced load flow and test algorithms on a standard unbalanced distribution network, which provides a framework for their practical use. Much research on the optimal allocation of DERs still assumes a balanced network can be tested and a pure radial configuration, which are not practical [20,21]. In all, the contributions of this paper are as follows:

1. We formulate a PV allocation optimization problem with two objectives and operational constraints.
2. A simple yet efficient fixed-point method is implemented to solve unbalanced power flow, to embrace the three-phase unbalanced feature in distribution networks.
3. A comparison is presented of several EAs, demonstrating their effectiveness in complex MINLP.

The rest of the paper is organized as follows: Section 2 formulates the PV allocation problem and then this is followed by the fixed-point method. Section 3 describes the methodology and implementation of EAs. Section 4 presents a case study with EAs and a comparative analysis. Finally, Section 5 concludes the paper with recommendations for future works.

2. Problem Formulation

Conventionally, a vector is represented by bold regulator letters such as v and a matrix is represented by italic capital letters, e.g., M. A scaler is written as a regular italic letter such as s. Multiplication is written as "$\times$" or "$\cdot$", or else it is omitted. Unless we specify otherwise, these conventions are adopted throughout this paper.

In this section, we first introduce an efficient iterative load flow (LF) method (i.e., the fixed-point method) used in the distribution network, followed by the optimal power flow (OPF) formulation, to represent the optimal PV allocation problem. The LF method is applied to enforce equality constraints in the OPF, which is highly non-linear. The problem consists of two objectives with certain constraints under PV-peak-hour operation (12:00 p.m.).

2.1. Distribution Power Flow (DPF)

The power flow program was first developed in the 1950s for transmission systems, and yet it did not become popular until the 1990s [22]. Distributed power flow analysis is the computational procedure used to determine the steady-state operation of the power system; in other words, to calculate the state variables of bus voltage magnitude and angle at each node.

Traditionally, the power flow in the distribution network is one-way from substation to loads, and yet, with high DER penetration into distribution networks, nowadays, the power flow direction can be bilateral, as demonstrated in Figure 1. IEEE1547-2018 is the standard that was released in 2018 to facilitate high DER penetration [3]. Advanced applications such as (1) voltage quality analysis (sizes and locations of capacitor banks, locations and ratings of voltage regulators, line upgrades), (2) DER integration (given the location of a new DER, determine the impact on operations), and (3) outage restoration analysis (if an outage occurs, determine how to operate switches to restore the load) are built upon DPF.

There are several popular power flow algorithms in the literature, and in this study, we implemented a simple yet efficient iterative method, the fixed-point method, which can handle heavily unbalanced and large DER-penetrated distribution circuits. Before introducing the fixed-point method, we list some disadvantages of two popular algorithms. (1) The backward/forward sweep method. Here, the first drawback is that this method can have trouble dealing with systems that have high penetration of distributed generation sources because, in this situation, the power flow might not be unidirectional, which violates an assumption of the method. The second drawback is that while it is relatively

efficient for smaller systems, the computational time can grow rapidly for large-scale, multi-phase, and unbalanced distribution systems. (2) The Newton Raphson method. In this case, the first drawback is that the Jacobian matrix used in this method needs to be updated and inverted at each iteration, which is computationally intensive, particularly for large-scale power systems. The second drawback is that the Newton Raphson method is most suited to transmission systems (generally mesh networks) and can have trouble with the unique characteristics of distribution systems, which are typically radial and have more unbalanced loads.

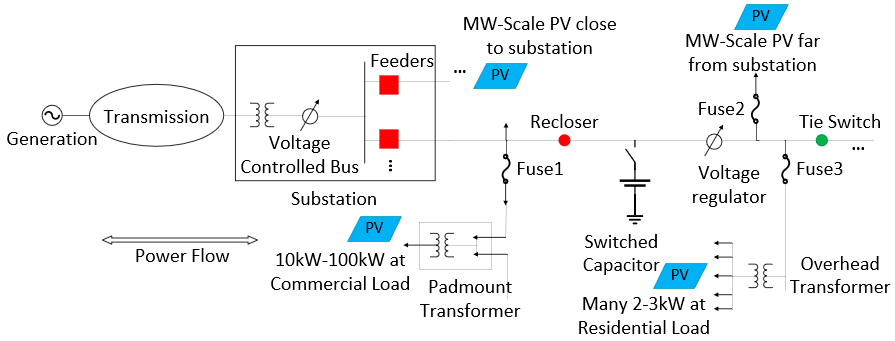

Figure 1. Distribution network with high PV penetration.

Therefore, this work adopted the fixed-point method operated in OpenDSS [7]. The mathematical process is presented here, followed by a summary of its advantages.

$$\mathbf{i}_{inj}(\mathbf{v}) = Y_{system} \times \mathbf{v} \tag{1}$$

Here, $\mathbf{i}_{inj}(\mathbf{v})$ is the compensation or injection current vector from the power conversion elements (load, generator, Vsource, Isource, storage, etc.) in the circuit, which may be non-linear, non-constant, and node-voltage dependent; $\mathbf{v}$ is the node voltage vector; and Y_{system} is a network admittance matrix composed of all elements' primitive matrices Y_{prim}, as shown in Figure 2.

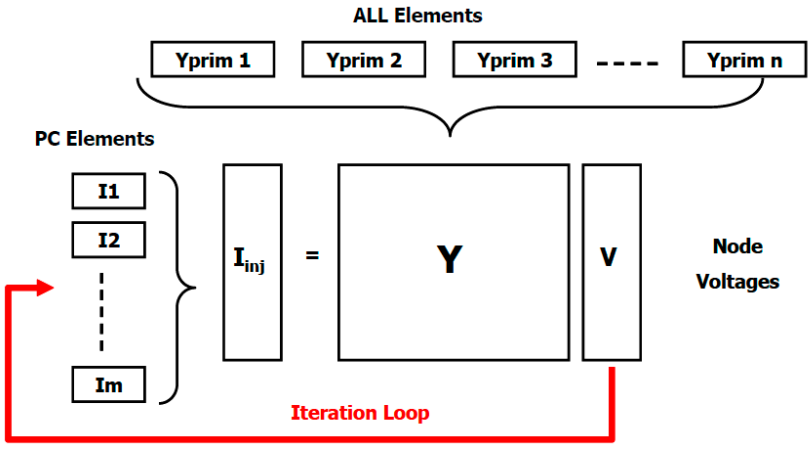

Figure 2. Fixed-point method.

Y_{prim} is the matrix representation for each current-carrying circuit element (lines, loads, regulators, capacitors, etc.). For example, to represent the relationship of a current with vector $\mathbf{i}$ and voltage vector $\mathbf{v}$ between two buses of two conductors, as shown in Figure 3, Y_{prim} is calculated and can be treated as a black box.

$$Z = \begin{bmatrix} z_{11} & m_{12} \\ m_{21} & z_{22} \end{bmatrix} \tag{2}$$

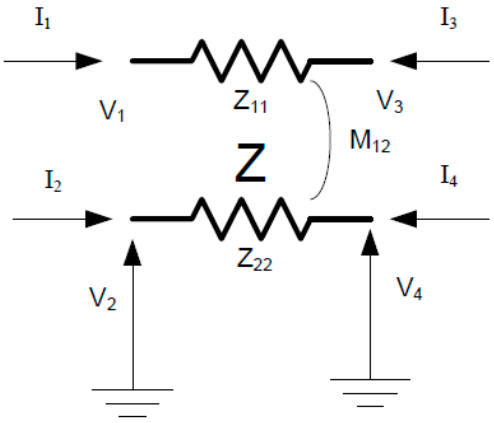

Figure 3. Primitive matrix illustration.

Here, v_1, v_2, v_3, and v_4 are voltages on terminals 1, 2, 3, and 4, respectively; Z is the self-impedance; and m is the mutual impedance induced by the magnetic field of two lines. Z is a 2 × 2 matrix describing the impedance characteristics of the coupled impedances. The element has four terminals, as shown in Figure 3, and a system of equations is written in nodal admittance form relating the currents entering each terminal to the voltage of each terminal with respect to a common zero-voltage reference, usually remote earth. The matrix relating the voltages and currents in this form is the Y_{prim} matrix as defined in (3) and (4). Note that the Z matrix appears four times in the Y_{prim} matrix. Lines, reactors, capacitor banks, and transformers of nearly any complexity can be modeled simply by extending the principles of this example to the actual number of phases and windings [7].

$$\begin{bmatrix} I_1 \\ I_2 \\ I_3 \\ I_4 \end{bmatrix} = \begin{bmatrix} Z^{-1} & -Z^{-1} \\ -Z^{-1} & Z^{-1} \end{bmatrix} \begin{bmatrix} V_1 \\ V_2 \\ V_3 \\ V_4 \end{bmatrix} \tag{3}$$

$$Y_{prim} = \begin{bmatrix} Z^{-1} & -Z^{-1} \\ -Z^{-1} & Z^{-1} \end{bmatrix} \tag{4}$$

As mentioned previously, the network Y_{system} admittance matrix is composed of the Y_{prim} of each circuit element, then an iterative method is used to solve $\mathbf{v}$. The process is straightforward. We first use an initial guess of $\mathbf{v}_0$ (1.0 p.u.) to calculate $\mathbf{i}_{inj}$ and then calculate the voltage iteratively until the algorithm converges (the difference in current and previous $\mathbf{v}$ is within a predefined threshold). Figure 4 presents a flow chart of the iterative PF method.

$$\mathbf{v}_{n+1} = Y_{system}^{-1} \times \mathbf{i}_{inj}(\mathbf{v}_n),\ n = 0,\ 1,\ 2,\ \ldots,\ n \tag{5}$$

Here, n is the number of iterations. Note that most entries in I are zero, but for DERs and non-linear voltage-dependent loads (such as constant power and constant current loads), the corresponding entries in I are non-zero. The advantages of this DLF are as follows: (1) Y_{system} remains constant if there is no network topology change. In other words, the matrix inversion only needs to be performed once during the iteration, which saves a lot of computational time. (2) The DLF can take very unbalanced three-phase networks and converge those successfully. (3) It is also suitable for parallel source (mesh topology) networks, as opposed to the radial network topology, which is required by the commonly used backward/forward sweep method [23]. (4) It provides the option to run a long-time-series continuous load flow efficiently thanks to the fast solving feature.

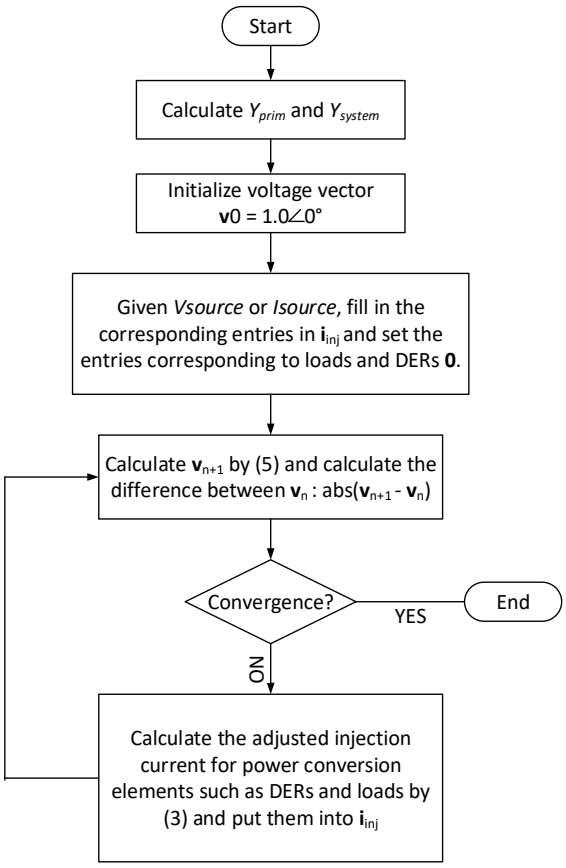

Figure 4. Flow chart of the iterative method.

2.2. Optimal PV Allocation

Figure 1 gives an overview of high PV system penetration into an unbalanced distribution network. This indicates that there are MW-scale, commercial, and residential types of PV systems and the power flow becomes bidirectional after large PV penetration. Bidirectional power flow certainly increases the complexity for system operators, but what is more concerning is the voltage issue introduced by PV. During the heavy loading period, PV penetration normally helps improve the voltage profile because voltage under a heavy load is near to or even lower than the low voltage limits. Thanks to PV penetration, the voltage will be boosted to the acceptable range. Yet, during light loading and high PV penetration times, such as noon, voltages are likely to be boosted above the high limit, which causes damage to the system.

Therefore, the PV allocation problem requires finding the optimal locations and sizing of PV systems to achieve objectives such as maximizing PV power injection or minimizing voltage deviation from 1.0 p.u. for all node voltages and when subjected to certain equality and inequality constraints. The mathematical form is expressed as follows:

$$\min f(\mathbf{u}) \tag{6}$$

$$g(\mathbf{u}, \mathbf{x}, \mathbf{y}) \leq 0 \tag{7}$$

$$h(\mathbf{u}, \mathbf{x}, \mathbf{y}) = 0 \tag{8}$$

where $\mathbf{u}$ is the control variable including PV locations and sizes; $\mathbf{x}$ is the state variable/dependent variable including voltages and angles at each bus; $\mathbf{y}$ is the known network parameters, such as network resistance, impendence, device rating, etc.; $g(\cdot)$ is the inequality constraints, which include line flow limit, voltage limit, and PV active power injection

limit; and $h(\cdot)$ represents the equality constraints, which constitute the power balance equation at each node, represented as follows:

$$\begin{aligned} P_i &= V_i \sum_{j=1}^{N} V_j Y_{ij} \cos(\delta_i - \delta_j - \theta_{ij}) \\ Q_i &= V_i \sum_{j=1}^{N} V_j Y_{ij} \sin(\delta_i - \delta_j - \theta_{ij}) \ \forall i, \forall j \end{aligned} \tag{9}$$

where P_i and Q_i are the real and reactive power at each node I. Note that unlike a transmission network, each bus in a distribution network will have to include multiple nodes in the model to reflect the possible unbalanced power flow. In other words, the size of equations increases significantly. V_i, V_j, δ_i, and δ_j, are the voltage magnitude and angle at nodes I and j; Y_{ij} and θ_{ij} are the Y-bus admittance matrix elements between nodes i and j. Equation (9) comprises two highly non-linear equations.

For the objective function $f(\cdot)$, two objectives, f_1 and f_2, were considered in this study. f_1 was to minimize the voltage violation while maximizing the power injection (minimizing negative power injection) at a specific hour, whereas f_2 was to minimize the voltage violation and voltage deviation from 1.0 p.u. at specific hour, as shown below:

$$f_1 = \sum_{i=1}^{n_{PV}} -p_{PVi} \tag{10}$$

$$f_2 = \sum_{i=1}^{n} \alpha \times |v_i - 1| \tag{11}$$

where v_i and p_{PVi} are the bus voltage and the real power injection at PV bus i, respectively; n_{pv} is the number of PV systems; n is the total number of buses; and the voltage deviation is multiplied by a constant number α of 1000. This will give the fitness value of the cost function of f_2 as a large number for clear selection and presentation.

As mentioned previously, $g(\cdot)$ are the inequality constraints, listed as follows:

$$p_{Gi,\min} \leq p_{Gi} \leq p_{Gi,\max} \tag{12}$$

$$t_{i,\min} \leq t_i \leq t_{i,\max} \tag{13}$$

$$v_{i,\min} \leq v_i \leq v_{i,\max} \tag{14}$$

$$S_{Li} \leq S_{Li,\max} \tag{15}$$

$$p_{pv,\min} \leq p_{pvi} \leq p_{pv,\max} \tag{16}$$

where (12) is the constraint for the i^{th} generator; (13) represents the i^{th} transformer tapping limit; (14) is the voltage limit at the i^{th} node; (15) is the complex power flow limit at the i^{th} line; and (16) represents the PV system capacity limits, which are 2000–20,000 kVA in this study. (16) is the control variable constraint, which is enforced within the control variable feasible domain. The rest of the equations are related to dependent variables, and only violations from (14) are penalized with objective functions, if they exist, because (12), (13),

and (15) are enforced when performing the power flow calculation in (5). The objective function then becomes (17):

$$f_{obj} = f + pen \times \sum_{i=1}^{n} \begin{cases} (v_i - v_{i,\max})^2 & v_i > v_{i,\max} \\ (v_{i,\min} - v_i)^2 & v_i < v_{i,\min} \\ 0 & \text{otherwise} \end{cases} \quad (17)$$

where f_{obj} is the final objective function including the penalization term, f is the objective functions defined from (10) and (11), and pen is a large positive number as the penalty coefficient.

3. Methodologies

Evolutionary algorithms (EAs) have proven effectiveness for complex optimization problems, many of which are in the energy domain [8,14]. In this work, several population-based evolutionary algorithms, ABC, PSO, DE, ABC-OL, and PSO-OL (integrated with orthogonal learning [8]), are implemented and compared to evaluate their effectiveness. The basic ABC and PSO have been proven effective and implemented in various real-world optimization problem scenarios like scheduling problems, financial modeling, resource allocation, etc., thanks to their features such as ease of implementation, adaptability, good balance of exploration and exploitation, etc. [8,24–28]. Thus, they were chosen as benchmarks, and future work can be focused on developing improved EAs to tackle these problems. The famous no free lunch theorem states that no meta-heuristic algorithm can be superior to the other algorithms for all optimization problems universally. Therefore, one of the objectives of this work was to extract their characteristics via a detailed comparative study.

3.1. Solution Vector

The EA solution vector structure is demonstrated in Figure 5. The control variables consist of location as the discrete variable and size as the continuous variable for peak-hour planning.

Variable Name	Type	Bounds	Dimension
(1) Location	Discrete	All 3-phase bus	Number of PVs
(2) Size	Continuous	2000-20,000kW	Number of PVs

$\mathbf{x} =$

Location 1	Size 1	Location 2	Size 2	...	Location n	Size n

Figure 5. EA solution vector structure.

3.2. Artificial Bee Colony in PV Allocation

The ABC is a population-based search algorithm mimicking the foraging of honeybees. Bees are sent out to randomly search in multidimensional feasible space (bounded by limits) to look for food sources (solutions) [29].

At initialization, each solution vector $\mathbf{u}_i = \{u_{i1}, u_{i2}, \ldots, u_{id}\}$ is generated randomly within the limits of the variables as follows:

$$u_{i,j} = u_{i,j\_\min} + rand(0,1) \times \left(u_{i,j\_\max} - u_{i,j\_\min}\right) \quad (18)$$

where u_{i,j_min} and u_{i,j_max} are the lower and upper bounds for the j^{th} dimension of the i^{th} food source, respectively. Note that there is a total n number of food sources (solutions) and d control variables and rand (0,1) is a random number within (0,1) obtained by assuming a uniform distribution.

Every food source will be updated to a new candidate solution based on the neighborhood's information. The nectar of new solutions (fitness value) will be evaluated to decide whether the current solution is to be replaced by the new one. Such selection is known as "greedy selection". The overall process is demonstrated in Figure 6 and Table 1.

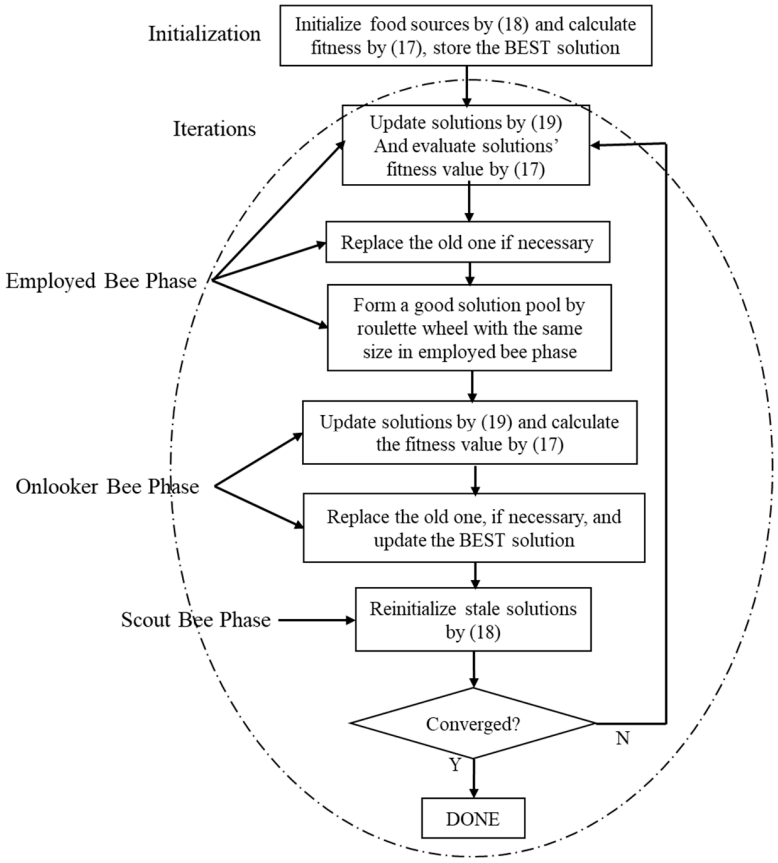

Figure 6. The overall ABC structure.

Table 1. Pseudocode for ABC.

Algorithm 1: ABC

Initialization:
  Set number of food sources (solutions), max iteration, max trial counter.
  Initialize the optimization variables (location and size) in the solution domain:
  $u_{i,j} = u_{i,j\_min} + rand(0,1) \times \left(u_{i,j\_max} - u_{i,j\_min}\right)$—Equation (18)
Repeat iteration t:
  Employed Bee Phase:
    for i = 1 to employed bee n
      $v_{i,j} = u_{i,j} + rand(-1,1) \times \left(u_{i,j} - u_{k,j}\right)$—Equation (19)
      Enforce the new candidate solution vector $\mathbf{v}_i$ within feasible limits.
      Evaluate the new solution and return its fitness value by (17).
      Apply greed selection between the new solution $\mathbf{v}_i$ and the original one $\mathbf{u}_i$
    end for
  Onlooker Bee Phase:
    for i = 1 to onlooker bee n
      Select a solution (solutions with better fitness values have higher probability to be selected).
      Modify the solution using (19).
      Enforce the new candidate solution vector $\mathbf{v}_i$ within feasible limits.
      Evaluate the new solution and return its fitness value by (17).
      Apply greedy selection between the new solution $\mathbf{v}_i$ and the original one $\mathbf{u}_i$.
    end for
  Scout Bee Phase:
    Abandon the food source (solution) whose trial counter is above the limit.
    Replace the abandoned food source with a new randomly generated one by (18).
  Memorize the best solution: record the best solution so far at each iteration.
Until termination criterion is met and output results.

The updated equation for a new candidate solution vector $\mathbf{v_i}$ is defined as follows:

$$v_{i,j} = u_{i,j} + rand(-1,1) \times \left(u_{i,j} - u_{k,j}\right) \tag{19}$$

where k is a different integer to i, which is randomly chosen from the size of the employed bees (n), and rand (−1,1) is a random number from (−1,1).

3.3. Particle Swarm Optimization in PV Allocation

The PSO is also a population-based search algorithm introduced by Kennedy and Eberhart in 1995 to explore the search space by using particles [24]. One particle consists of velocity and position, where position is the feasible solution updated with the help of the previous position and velocity, as shown below:

$$\mathbf{v}_i^{new} = \omega_I \mathbf{v}_i + r_1 \omega_M (\mathbf{b}_i - \mathbf{x}_i) + r_2 \omega_C (\mathbf{b}_G - \mathbf{x}_i) \tag{20}$$

$$\boldsymbol{x}_i^{new} = \mathbf{x}_i + \mathbf{v}_i^{new} \tag{21}$$

where ω_I, ω_M, and ω_C are the weights for inertia, memory, and cooperation terms; r_1 and r_2 are two random numbers from 0 to 1; b_i and b_G are the personal best and global best; $\mathbf{x}_i^{new}$ is the new solution computed with the help of $\mathbf{v}_i^{new}$ for the i^{th} population. Figure 7 shows a flow chart of PSO for PV allocation, and pseudocode for PSO is given in Table 2.

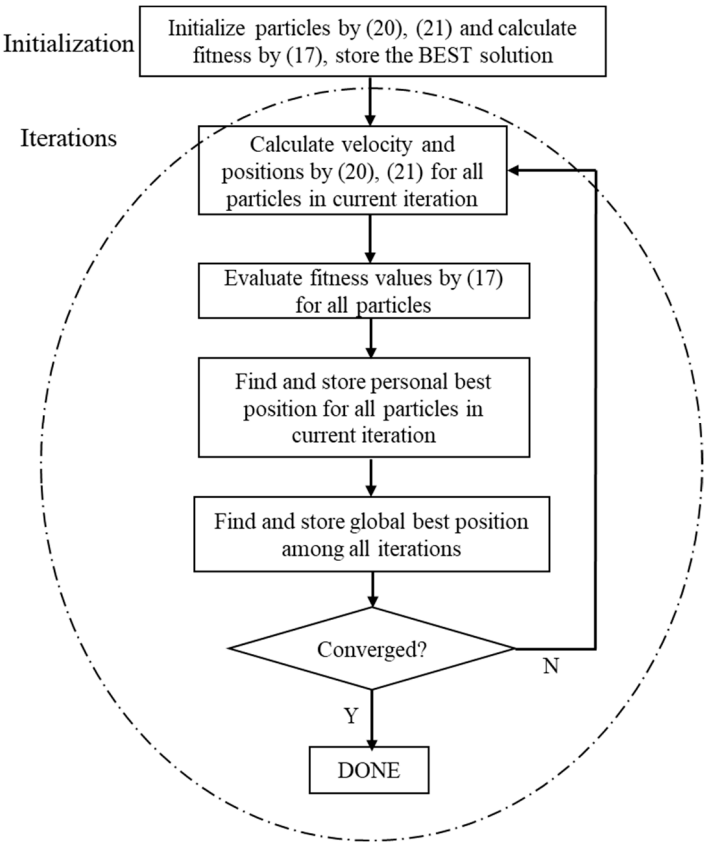

Figure 7. The overall PSO structure.

As mentioned, both ABC and PSO are known for their efficiency in solving complex real-world optimization problems. The main idea is that swarms are sent out to search for the near-optimal solution based on intelligent mechanisms mimicking the biological behaviors in a non-convex and non-linear solution domain. To ensure successful applications, the key is to evaluate the solution and return a fitness value. For real-world problems, as long

as there is a mechanism (mathematical model, neural network, fuzzy system, etc.) with which to evaluate the solution, it is worthwhile assessing the performances of ABC and PSO in solving the problems.

Table 2. Pseudocode for PSO.

Algorithm 2: PSO

Initialization:
  Set parameters such as max iteration, population size n, ω_I, ω_M, ω_C, r_1, and r_2.
  Initialize population $\mathbf{x}$ (solutions) in the feasible domain.
  Evaluate the solutions and return their fitness value by (17).
  Set each particle's personal best $\mathbf{b}_i$ equal to current particle $\mathbf{x}_i$.
  Set the global best $\mathbf{b}_G$ equal to the best particle $\mathbf{x}_i$ that corresponds to the minimal fitness value.
Repeat iteration t
    for i = 1 to population size n
      $\mathbf{v}_i^{new} = \omega_I \mathbf{v}_i + r_1 \omega_M (\mathbf{b}_i - \mathbf{x}_i) + r_2 \omega_C (\mathbf{b}_G - \mathbf{x}_i)$—Equation (20)
      $\mathbf{x}_i^{new} = \mathbf{x}_i + \mathbf{v}_i^{new}$
    end for
    Enforce $\mathbf{X}_i^{new}$, $\mathbf{V}_i^{new}$ within feasible limits.
    Evaluate the new solution $f(\mathbf{X}_i^{new})$ and return its fitness value by (17).
    Update the personal best $\mathbf{b}_i$.
    Update the global best $\mathbf{b}_G$.
Until termination criterion is met
Return *global best*

For this comparative study, we also implemented DE, ABC-OL, and PSO-OL (OL stands for orthogonal learning) for optimal PV allocation. It was interesting to find that DE, which is known for its efficiency in solving continuous optimization problems, failed to present any feasible solutions for the two objectives in the IEEE-13 and -37 test beds. We propose that the reason for its failure concerned the nature of the problem, where half of the optimization variables are discrete. Given its failure, we exclude the results for DE from Section 4. Furthermore, the OL concept and its integration into ABC and PSO can be found in [8,30] in detail; as such, due to space constraints, we do not present the implementation here.

4. Results and Discussions

This section first describes case studies where three-phase PV systems are to be installed in the IEEE-13 and -37 bus systems to achieve two objectives, and this is followed by a performance analysis and discussion. Three-phase PV systems are adopted here to ensure successful power flow, because if we were to consider single- or two-phase buses used to install large PV systems, those systems could become very unbalanced to the point where huge violations could occur, causing the power flow to diverge. Note that the potential buses used to install PV systems are three-phase 4.16 kV and 4.8 kV levels for the IEEE-13 and -37 bus systems, respectively. Table 3 summarizes all cases and scenarios in this study. The PC used for simulation has 32 G RAM and an 11th Gen Intel Core i7 processor.

Table 3. Cases and scenarios.

	Case 1: Maximum PV Penetration	**Case 2: Minimum Voltage Deviation**
IEEE-13 Scenario 1	one PV system's optimization	one PV system's optimization
IEEE-13 Scenario 2	two PV systems' optimization	two PV systems' optimization
IEEE-37 Scenario 3	one PV system's optimization	one PV system's optimization
IEEE-37 Scenario 4	two PV systems' optimization	two PV systems' optimization

4.1. PV and Load Profile

For this work, a three-phase PV system rated at 4.16 kV, with a possible output of 2000–20,000 kVA and a power factor of 1, was chosen. The PV system was installed optimally in IEEE-13 and IEEE-37 bus circuits to evaluate the EAs' performance. Note that even though the PV system is three-phase, the circuit itself is an unbalanced network, which brings many challenges for planning. Figure 8 gives the load profile in p.u. of the chosen date. Figure 9 shows the temperature and PV output in p.u. for the selected date. Clearly, the PV output has a positive correlation with the temperature. For this study, only the loading condition and PV output from 12:00 pm were utilized, as the objectives from (10) and (11) were to obtain the optimal allocation considering the peak hour PV output, which was assumed to occur at noon.

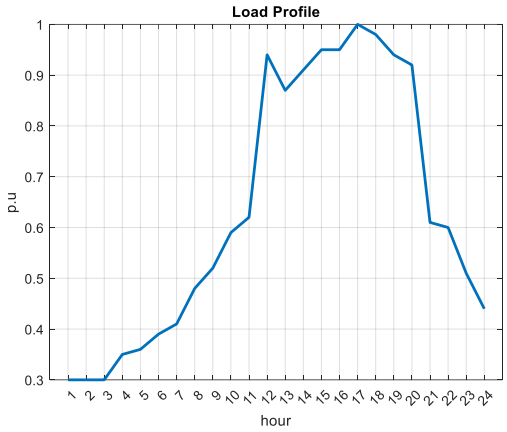

Figure 8. Load profile.

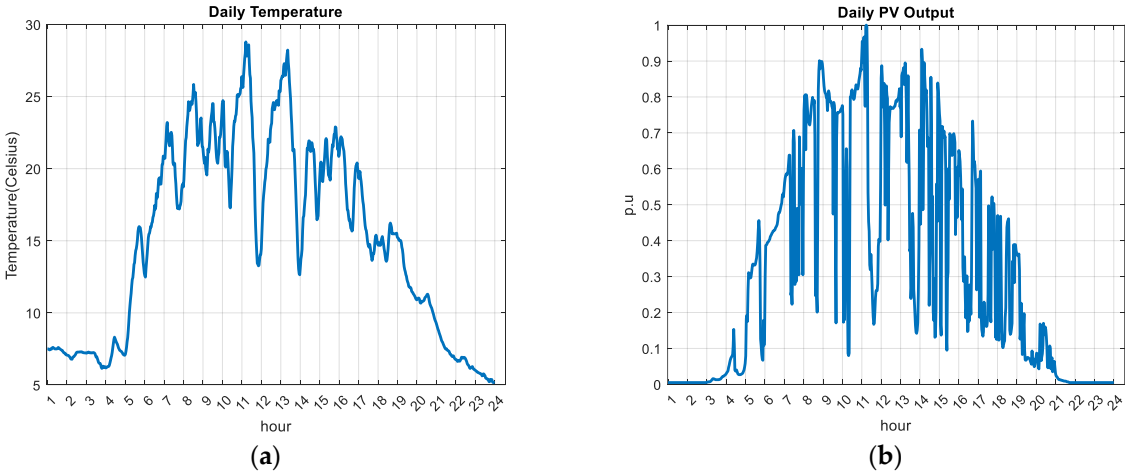

Figure 9. Temperature (**a**) and PV output (**b**).

4.2. PV Penetration Maximization on IEEE-13 and -37 Bus Test Systems

The objective of this case study was to maximize the PV penetration. The first and second scenarios were conducted on the IEEE-13 bus system. The potential buses used to interconnect PV systems were {670, 671, 633, 680, 675, 692}, as shown in Figure 10a. The third and fourth scenarios were conducted on the IEEE-37 bus system, as shown in Figure 10b. The potential buses used to interconnect PV systems were {701, 702, 703, 704, 705, 706, 707, 708, 709, 710, 711, 712, 713, 714, 718, 720, 722, 724, 725, 727, 728, 729, 730, 731, 732, 733, 734, 735, 736, 737, 738, 740, 741, 742, 744}, and the possible PV size was from 2000 to 20,000 kVA for both test cases. To become a potential location, the rated bus voltage was required be at 4.16 kV and a three-phase bus was needed.

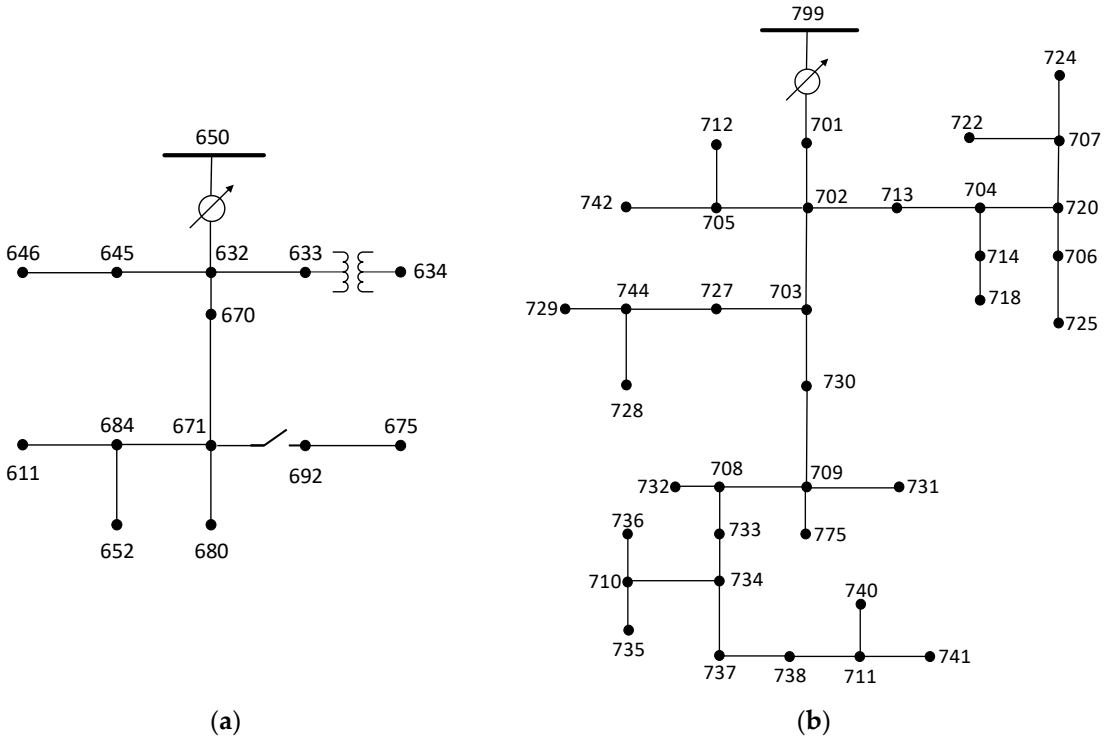

Figure 10. IEEE-13 (**a**) and -37 (**b**) bus test systems.

Table 4 shows the results of the 30-run experiment. The column "Solution" presents the optimal solution found with evolutionary algorithms in 30 runs, which indicates the bus location and kVA injection size. "Min", "Avg", "Max", and "Std" represent the minimum, average, maximum, and standard deviation of the fitness values, respectively. A negative fitness value means the solution (location and size of PV system) did not lead to voltage violation. Alternatively, a positive fitness value means the solution introduced voltage violation in (16). The column "FE" indicates the function evaluations at one run. In EAs, function evaluation is the critical process followed to calculate the fitness value (cost in objective functions). "#pop/iterations" represents the population size corresponding to the total iterations of the algorithm. To ensure equity in comparison, we set those values equally.

Table 4. Maximizing PV penetration on the IEEE-13 bus system.

	One PV System Allocation							
	Min	Avg	Max	Std	T(s)	FE	Solution (Bus, kVA)	#pop/iterations
ABC	−14,528	−14,526	−14,522	1.2	6	20247	(670, 14,526)	100/200
ABC-OL	−14,528	−14,526	−14,525	0.8	21	36236	(670, 14,527)	100/200
PSO	−14,528	−14,527	−14,525	0.6	6	20100	(670, 14,528)	100/200
PSO-OL	−14,526	−14,525	−14,521	1.3	24	20100	(670, 14,526)	100/200
	Two PV systems allocation							
	Min	Avg	Max	Std	T(s)	FE	Solution (Bus, kVA)	#pop/iterations
ABC	−15,787	−15,708	−15,520	70.1	7	20,249	(633, 5080; 670, 10,591)	100/200
ABC-OL	−15,779	−15,701	−15,520	69.1	22	52,189	(633, 4786; 670, 10,957)	100/200
PSO	−15,797	**−15,796**	−15,792	1.5	7	20,100	(633, 4965; 670, 10,832)	100/200
PSO-OL	−15,796	−15,795	−15,788	1.5	24	20,100	(633, 4967; 670, 10,829)	100/200

It can be noted from the one PV system allocation that all EAs could find similar solutions regarding "Min", "Avg", "Max", and "Std". PSO achieved this with the least computing time. This implied that the problem was relatively simple and most EAs could

find the solution efficiently and robustly (low standard deviation). For the two PV system allocation, it can be noted that the best solution in "Avg" was found by using PSO, and it was also the most efficient solution (least time consumed). Furthermore, the "Std" results found by ABC and ABC-OL were much larger than those from PSO and PSO-OL, which implied less robustness.

Figure 11 shows convergence plots for the four algorithms based on the one PV and two PV system allocations. In both plots, the four algorithms can be seen to have found similar results efficiently, which implies a simple structure for the problem. Yet, PSO and its variant PSO-OL had faster convergence rates for the problem. It can also be noted from the zoomed-in image that the convergence rates in the one PV and two PV cases were the same from fast to slow: PSO-OL, PSO, ABC, and ABC-OL.

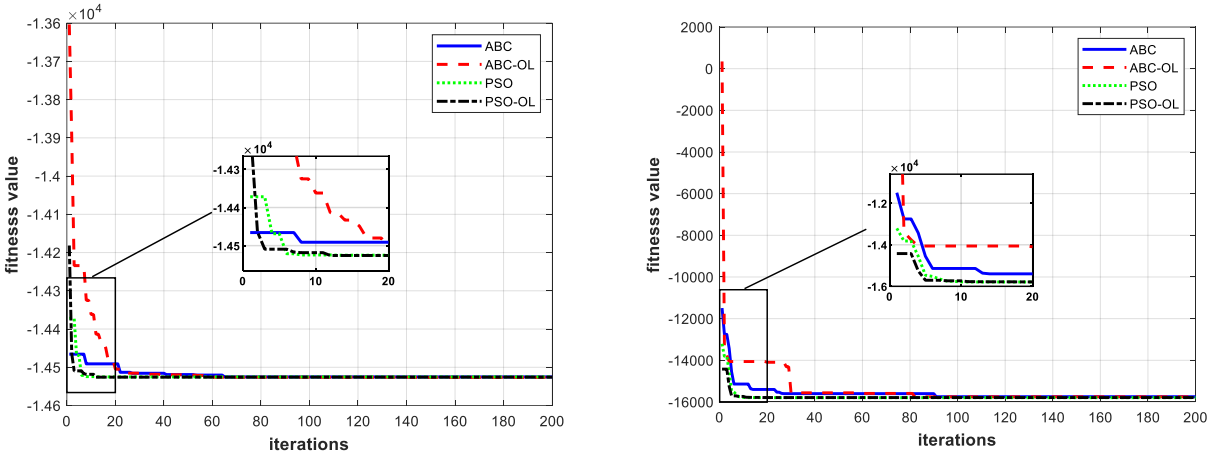

Figure 11. Convergence plots for the one PV system (**a**) and two PV systems (**b**) optimal allocations on the IEEE-13 bus system.

Table 5 shows the results found with the four algorithms in the IEEE-37 bus system over 30 runs. It can be noted that the solution found with PSO has the lowest fitness value in "Avg" for both cases. Furthermore, the "Std" result for this scenario is relatively large compared with that for the IEEE-13 bus system, which implies that the complexity of the problem has increased significantly.

Table 5. Maximizing PV penetration in the IEEE-37 bus system.

	One PV System Allocation							
	Min	Avg	Max	Std	T(s)	FE	Solution (Bus, kVA)	#pop/iterations
ABC	−8804	−8493	−8089	172	17	16,232	(705, 8296)	80/200
ABC-OL	−9004	−8406	−8071	196	35	29,336	(714, 8351)	80/200
PSO	−8938	**−8590**	−8060	195	21	16,080	(705, 8938)	80/200
PSO-OL	−8724	−8244	−7544	420	34	16,080	(705, 8724)	80/200
	Two PV systems allocation							
	Min	Avg	Max	Std	T(s)	FE	Solution (Bus, kVA)	#pop/iterations
ABC	−28,769	−28,194	−27,801	213	26	16,233	(705, 8201; 740, 20,000)	80/200
ABC-OL	−28,645	−27,991	−27,659	255	40	42,219	(727, 7825; 724, 20,000)	80/200
PSO	−28,620	**−28,274**	−27,506	215	20	16,080	(714, 8624; 727, 20,000)	80/200
PSO-OL	−28,416	−26,537	−26,026	270	43	16,080	(713, 9035; 733, 20,000)	80/200

Figure 12 shows convergence plots for the four algorithms based on the one PV and two PV system allocations. In the left-hand plot, even though the convergence rates and results are similar for all algorithms, PSO and PSO-OL have particularly good initial solutions. In the right-hand plot, PSO has the fastest convergence rate, yet PSO-OL seems to

become trapped at the local minima in early iterations and barely improves in the following iterations.

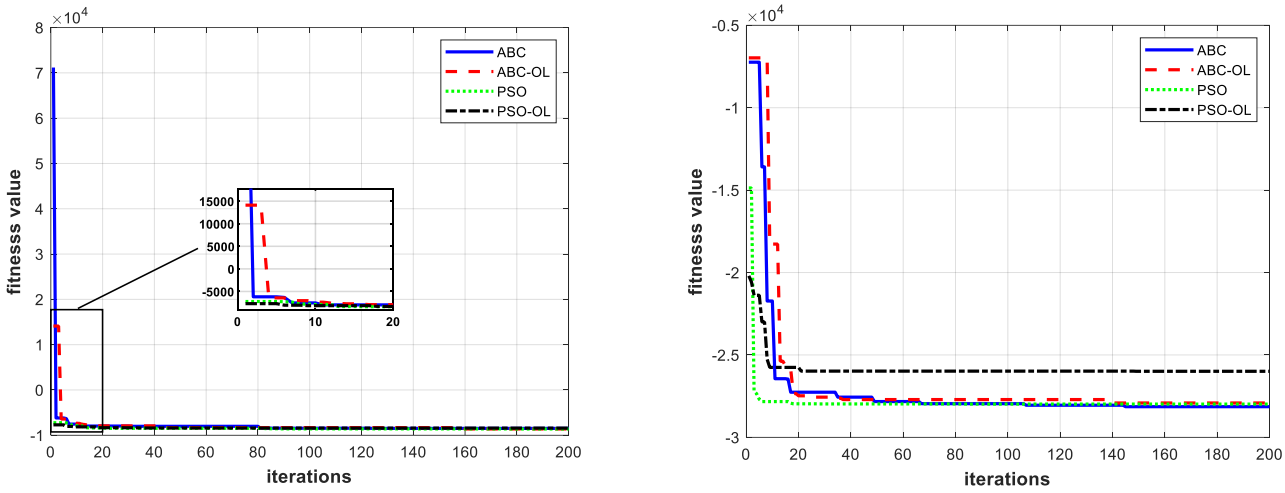

Figure 12. Convergence plots for the one PV system (**a**) and two PV systems (**b**) optimal allocations in the IEEE-37 bus system.

From case 1, it can be observed that basic PSO is the most effective EA for optimal PV allocations when considering maximum PV penetration and when seeking to find solutions with the lowest average cost. The fast convergence rate also demonstrates its effectiveness.

4.3. Voltage Deviation Minimization in the IEEE-13 and -37 Bus Test Systems

In this case, the PV systems to be installed and the potential buses in the test circuits are the same as those described in Section 4.2. Table 6 shows the results for the IEEE-13 bus system over 30 runs. The fitness value (objective cost) for this case is always a positive value since the cost is added whenever voltages are beyond the limits and deviating by over 1.0 p.u. from Equation (10). It is worth noting that for both the one PV and two PV allocation scenarios, the results obtained with the four algorithms are consistent and robust. This implies that the problem is relatively simple, such that EAs can search in the solution domain efficiently to obtain consistent "optimal" solutions.

Table 6. Minimizing voltage deviation in the IEEE-13 bus system.

	One PV System Allocation							
	Min	Avg	Max	Std	T(s)	FE	Solution (Bus, kVA)	#pop/iterations
ABC	535	535	535	0.1	4	12,184	(670, 10,649)	60/200
ABC-OL	535	535	535	0.1	9	21,692	(670, 10,632)	60/200
PSO	535	535	535	0.1	4	12,060	(670, 10,689)	60/200
PSO-OL	535	535	535	0.1	9	7375	(670, 10,654)	60/200
	Two PV systems allocation							
	Min	Avg	Max	Std	T(s)	FE	Solution (Bus, kVA)	#pop/iterations
ABC	455	455	456	1	6	12,127	(633, 4920; 692, 4474)	60/200
ABC-OL	455	455	455	0.1	9	31,314	(633, 5279; 692, 4320)	60/200
PSO	455	456	484	5	4	12,060	(633, 5119; 692, 4392)	60/200
PSO-OL	455	455	455	0.1	10	7416	(633, 5382; 692, 4275)	60/200

Figure 13 shows convergence plots for the four algorithms based on the one PV and two PV system allocations. These plots reveal that the four algorithms could find similar results efficiently, which implies a simple structure for the problem. Yet, in the right-hand plot, PSO-OL has the lowest convergence rate.

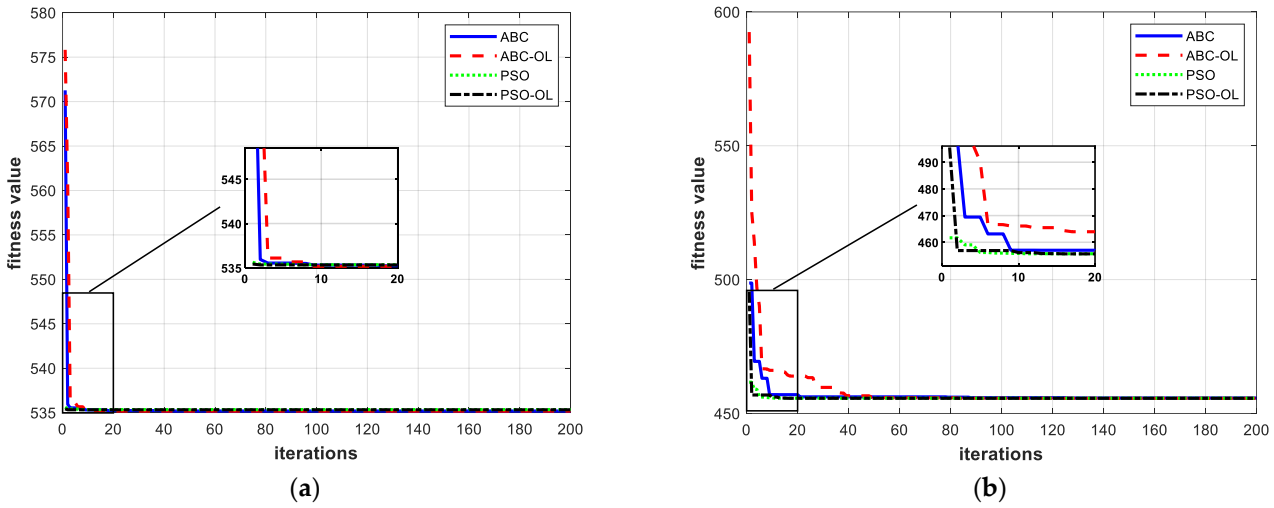

Figure 13. Convergence plots for the one PV system (**a**) and two PV systems (**b**) optimal allocations in the IEEE-13 bus system.

Since the objective is to minimize voltage deviation, the optimal voltage profiles solved with PSO are listed in Figure 14. There are a total of 41 node voltages for the IEEE-13 bus unbalanced three-phase distribution network, because each bus can have multiple nodes. It can be observed that the voltage profiles are greatly improved for both the one PV and two PV system optimal allocations.

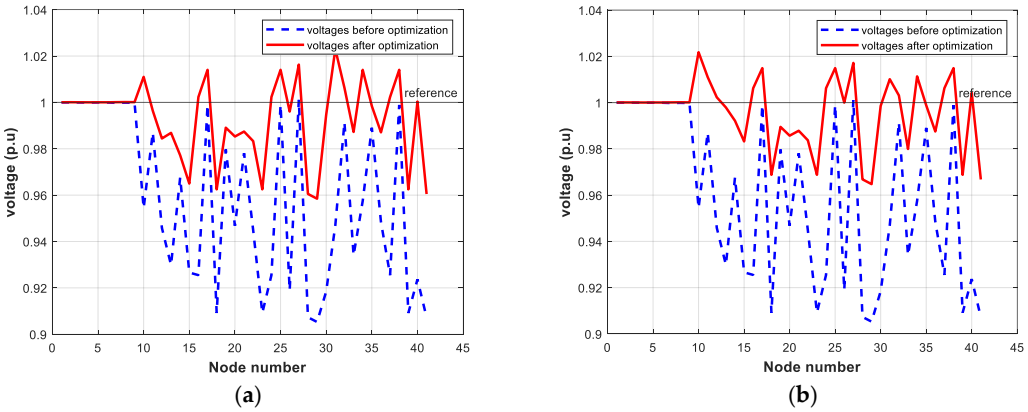

Figure 14. Voltage profiles for the one PV system (**a**) and two PV systems (**b**) optimal allocations in the IEEE-13 bus system.

Table 7 shows the results for the IEEE-37 bus system. ABC and ABC-OL outperformed PSO-based algorithms in the "Min", "Avg", "Max", and "Std" attributes. Specifically, ABC-OL found the solutions with the least cost in "Avg" for both the one PV and two PV scenarios. Yet, ABC-OL required more computing time. It is also interesting to see that in the two PV scenario, PSO-OL obtained the lowest "Std", which shows its robustness.

Figure 15 shows the corresponding convergence plots. There are a total of 500 iterations for all four algorithms, more than in the previous cases. In relation to this, it is worthwhile noting that "optimal" solutions are normally not found at an early stage. For example, in this study, ABC-OL in the left-hand plot does not converge until around the 160th iteration, nor does it converge until around the 110th iteration in the right-hand plot. Clearly, even though the PSO-based algorithms converge quickly, they are trapped at the local minimum and their solutions do not improve in later iterations. It can also be observed that for the one PV and two PV systems, the final results found with ABC and ABC-OL are similar, and the final results found with PSO and PSO-OL are also comparable.

Table 7. Minimizing voltage deviation in the IEEE-37 bus system.

	Min	Avg	Max	Std	T(s)	FE	Solution (Bus, kVA)	#pop/iterations
One PV System Allocation								
ABC	1062	1217	1363	85	75	50,538	(703, 7397)	100/500
ABC-OL	1062	**1105**	1260	69	86	90,505	(670, 10,556)	100/500
PSO	1367	1471	1600	114	73	50,100	(727, 7977)	100/500
PSO-OL	1091	1157	1389	77	87	30,267	(703, 7073)	100/500
Two PV systems allocation								
	Min	Avg	Max	Std	T(s)	FE	Solution (Bus, kVA)	#pop/iterations
ABC	1034	1181	1320	66	71	50,535	(727, 7632; 733, 11,219)	100/500
ABC-OL	1062	**1154**	1285	57	117	131,883	(703, 7289; 718, 9549)	100/500
PSO	1362	1372	1383	10	75	50,100	(727, 7818; 718, 16,404)	100/500
PSO-OL	1356	1367	1389	9	98	30,389	(727, 8059; 733, 14,353)	100/500

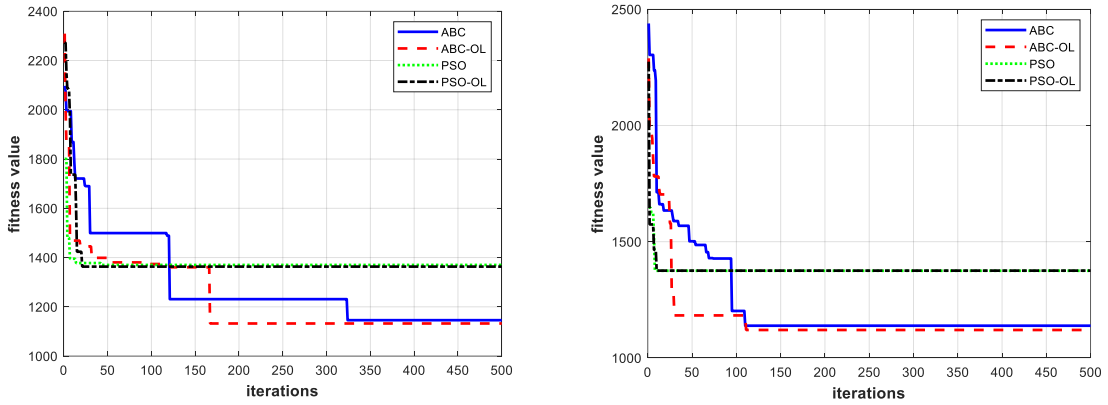

Figure 15. Convergence plots for the one PV system (**a**) and two PV systems (**b**) optimal allocations in the IEEE-37 bus system.

Similarly, the optimal voltage profiles found with ABC-OL are listed in Figure 16. There are a total of 117 node voltages for the IEEE-37 bus unbalanced three-phase distribution network. Note that the original circuit has a very poor voltage profile (blue dotted line), where most voltages of buses are lower than the voltage limit of 0.9 p.u. Such a voltage profile can cause significant damage to infrastructure. Yet, it can be observed that the voltage profile has been greatly improved for both the one PV and two PV system optimal allocations.

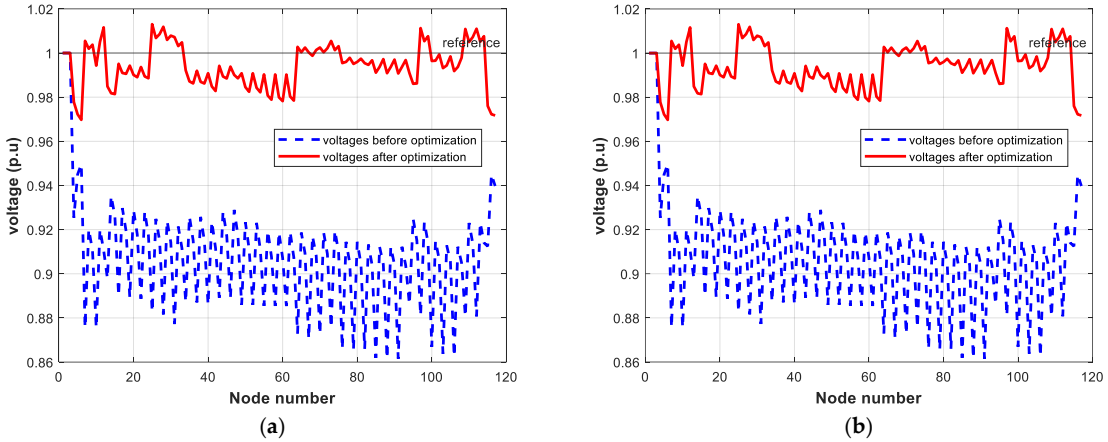

Figure 16. Voltage profiles for the one PV system (**a**) and two PV systems (**b**) optimal allocations in the IEEE-37 bus system.

5. Conclusions

Distribution networks have become active and complicated, containing bilateral power flow and large DER penetration. Finding the optimal locations and sizes of PV systems creates a complex planning problem, and solving that problem is critical for distribution network management. This work explored the possibility of using EAs (ABC, PSO, and their variants) to tackle such a problem with the help of a simple and yet efficient fixed-point iterative load flow method that ensures the unbalanced network will be solved successfully. All EAs were verified on IEEE-13 and -37 bus systems with two objectives (maximum PV penetration and minimum voltage deviation). After 30 runs, all EAs except for DE were relatively successful in finding solutions, but they had different attributes, such as the ability to find lower or stable fitness values. The ABC-related algorithms generally converged with better solutions and yet with statistically larger deviations in minimum voltage. Meanwhile, the PSO-related algorithms were more efficient in terms of maximum PV penetration. For the minimum voltage deviation case, the voltage profile was boosted by around 1.0 p.u. after optimization. Such a voltage profile will reduce infrastructural degradation significantly. This work proves the EAs' efficiency in solving such problems and highlights that they may realistically be used as tools for operators when planning the integration of PV systems into unbalanced distribution networks. Thus, this work can be considered a proof of concept for optimal PV system allocation problems. Nonetheless, it has its limits, such as the use of only up to two PV systems for peak-hour planning. Utilities will certainly want to optimally allocate more PV systems in a long period. Therefore, future work should focus on conducting day-ahead optimal planning using basic EAs and/or improved EAs, which should be applied to more PV systems. We wish to emphasize that from a practical perspective, the implementation of EAs for the optimal allocation of PV systems is a good approach because the problem does not require a real-time solution but just needs a better solution without that coming at the expense of computational cost. The source code is available publicly for researchers and practitioners to explore as part of efforts to extend this work.

Author Contributions: Conceptualization, W.B. and W.Z.; methodology, W.B. and R.A.; validation, W.B. and I.E.; writing—original draft preparation, W.B.; writing—review and editing, W.Z. and K.Y.L. All authors have read and agreed to the published version of the manuscript.

Funding: This research received no external funding.

Data Availability Statement: The data and MATLAB code are accessible at https://github.com/wbai123/Matlab-code-Optimal-PV-sizing-and-location-using-meta-heuristics-interacting-with-OpenDSS. Accessed on 1 September 2023.

Acknowledgments: This article is a revised and expanded version of a paper entitled "Optimal Allocation of PV Systems on Unbalanced Networks Using Evolutionary Algorithms", which was presented at the conference 2023 IEEE Symposium Series on Computational Intelligence (SSCI), Mexico City, Mexico, published on IEEEXplore on 1 January 2024.

Conflicts of Interest: The authors declare no conflicts of interest.

References

1. Downing, J.; Johnson, N.; McNicholas, M.; Nemtzow, D.; Oueid, R.; Paladino, J.; Wolfe, E.B. *Pathways to Commercial Liftoff: Virtual Power Plants*; U.S. Department of Energy Report 2023; U.S. Department of Energy: Washington, DC, USA, 2023.
2. Honarmand, M.E.; Hosseinnezhad, V.; Hayes, B.; Siano, P. Local energy trading in future distribution systems. *Energies* **2021**, *14*, 3110. [CrossRef]
3. IEEE Standard for Interconnection and Interoperability of Distributed Energy Resources with Associated Electric Power Systems Interfaces. Available online: https://standards.ieee.org/ieee/1547/5915/ (accessed on 8 August 2023).
4. Bawazir, R.O.; Cetin, N.S. Comprehensive overview of optimizing PV-DG allocation in power system and solar energy resource potential assessments. *Energy Rep.* **2020**, *6*, 173–208. [CrossRef]
5. Rajicic, D.; Ackovski, R.; Taleski, R. Voltage Correction Power Flow. *IEEE Trans. Power Deliv.* **1994**, *9*, 1056–1062. [CrossRef]

6. Karimi, M.; Shahriari, A.; Aghamohammadi, M.R.; Marzooghi, H.; Terzija, V. Application of Newton-based load flow methods for determining steady-state condition of well and ill-conditioned power systems: A review. *Int. J. Electr. Power Energy Syst.* **2019**, *113*, 298–309. [CrossRef]
7. Dugan, R.C.; McDermott, T.E. An open-source platform for collaborating on smart grid research. In Proceedings of the 2011 IEEE PES General Meeting, Detroit, MI, USA, 24–28 July 2011.
8. Bai, W.; Eke, I.; Lee, K.Y. An improved artificial bee colony optimization algorithm based on orthogonal learning for optimal power flow problem. *Control Eng. Pract.* **2017**, *61*, 163–172. [CrossRef]
9. Bienstock, D.; Chertkov, M.; Harnett, S. Chance-Constrained Optimal Power Flow: Risk-Aware Network Control under Uncertainty. *SIAM Rev.* **2014**, *56*, 461–495. [CrossRef]
10. Nammouchi, A.; Aupke, P.; D'Andreagiovanni, F.; Ghazzai, H.; Theocharis, A.; Kassler, A. Robust opportunistic optimal energy management of a mixed microgrid under asymmetrical uncertainties. *Sustain. Energy Grids Netw.* **2023**, *36*, 101184–101199. [CrossRef]
11. Acharya, N.; Mahat, P.; Mithulananthan, N. An analytical approach for DG allocation in primary distribution network. *Int. J. Electr. Power Energy Syst.* **2006**, *28*, 669–678. [CrossRef]
12. Abdelsalam, A.A.; El-Saadany, E.F. Probabilistic approach for optimal planning of distributed generators with controlling harmonic distortions. *IET Gener. Transm. Distrib.* **2013**, *7*, 1105–1115. [CrossRef]
13. Bai, W.; Zhu, X.; Lee, K.Y. Dynamic optimal power flow based on a spatio-temporal wind speed forecast model. In Proceedings of the 2021 IEEE Congress on Evolutionary Computation, Virtual, 28 June–21 July 2021; pp. 136–143.
14. Bai, W.; Abedi, M.; Lee, K.Y. Distributed generation system control strategies with PV and fuel cell in microgrid operation. *Control Eng. Pract.* **2016**, *53*, 184–193. [CrossRef]
15. Janamala, V.; Rani, K.R. Optimal allocation of solar photovoltaic distributed generation in electrical distribution networks using archimedes optimization algorithm. *Clean Energy* **2022**, *6*, 271–287. [CrossRef]
16. Kumawat, M.; Gupta, N.; Jain, N.; Bansal, R.C. Optimal planning of distributed energy resources in harmonics polluted distribution system. *Swarm Evol. Comput.* **2018**, *39*, 99–113. [CrossRef]
17. Nogueira, W.C.; Negrete, P.G.; Lezama, J.M. Optimal allocation and sizing of distributed generation using interval power flow. *Sustainability* **2023**, *15*, 5171. [CrossRef]
18. Wolpert, D.H.; Macready, W.G. No free lunch theorem for optimization. *IEEE Trans. Evol. Comput.* **1997**, *1*, 67–82. [CrossRef]
19. Bai, W.; Zhang, W.; Meng, F.; Allmendinger, R.; Lee, K.Y. Optimal Allocation of PV Systems on Unbalanced Networks Using Evolutionary Algorithms. In Proceedings of the 2023 IEEE Symposium Series on Computational Intelligence (SSCI), Mexico City, Mexico, 5–8 December 2023.
20. Albadi, M.; Soliman, H.; Thani, M.A.; Al-Alawi, A.; Al-Ismaili, S.; Al-Nabhani, A.; Baalawi, H. Optimal Allocation of PV Systems to Minimize Losses in Distribution Networks Using GA and PSO: Masirah Island Case Study. *J. Electr. Syst.* **2017**, *13*, 678–688.
21. Bai, W.; Eke, I.; Lee, K.Y. Optimal scheduling of distributed energy resources by modern heuristic optimization technique. In Proceedings of the 2017 19th International Conference on Intelligent System Application to Power Systems (ISAP), San Antonio, TX, USA, 17–20 September 2017.
22. Grisales-Norena, L.F.; Morales-Duran, J.C.; Velez-Garcia, S.; Montoya, O.D.; Gil-Gonzalez, W. Power flow methods used in AC distribution networks: An analysis of convergence and processing times in radial and meshed grid configurations. *Results Eng.* **2023**, *17*, 100915–100924. [CrossRef]
23. Gao, D.; Muljadi, E.; Tian, T.; Miller, M. *Software Comparison for Renewable Energy Deployment in a Distribution Network*; Technical Report; The National Renewable Energy Laboratory (NREL): Golden, CO, USA, 2017.
24. Eberhart, R.C.; Kennedy, J. A new optimizer using particle swarm theory. In Proceedings of the 6th International Symposium on Micro Machine and Human Science, Nagoya, Japan, 13–16 March 1995.
25. Houssein, E.H.; Gad, A.G.; Hussain, K.; Suganthan, P.N. Major Advances in Particle Swarm Optimization: Theory, Analysis, and Application. *Swarm Evol. Comput.* **2021**, *63*, 100868–100907. [CrossRef]
26. Pradeepkumar, D.; Ravi, V. Forecasting financial time series volatility using particle swarm optimization trained quantile regression neural network. *Appl. Soft Comput.* **2017**, *58*, 35–52. [CrossRef]
27. Sheikholeslami, F.; Navimipour, N.J. Service allocation in the cloud environments using multi-objective particle swarm optimization algorithm based on crowding distance. *Swarm Evol. Comput.* **2017**, *35*, 53–64. [CrossRef]
28. Bolaji, A.L.; Bamigbola, A.F.; Adewole, L.B.; Shola, P.B.; Afolorunso, A.; Obayomi, A.A.; Aremu, D.R.; Almazroi, A.A. A room-oriented artificial bee colony algorithm for optimizing the patient admission scheduling problem. *Comput. Biol. Med.* **2022**, *148*, 105850–105863. [CrossRef]
29. Karaboga, D. *An Idea Based on Honeybee Swarm for Numerical Optimization*; Technical Report TR06; Erciyes University, Engineering Faculty, Computer Engineering Department: Talas, Turkey, 2005.
30. Zhan, Z.H.; Zhang, J.; Li, Y.; Shi, Y.H. Orthogonal learning particle swarm optimization. *IEEE Trans. Evol. Comput.* **2011**, *15*, 832–847. [CrossRef]